LETTER

Mechanical response of polyprotein revealed by single-molecule optical tweezers

Applied Physics Express 15, 075002 (2022)
https://doi.org/10.35848/1882-0786/ac6a40

LETTER

Mechanical response of polyprotein revealed by single-molecule optical tweezers

Shuai Li[1,2], Haiqing Liu[3*], Chunguang Hu[2*], Chengzhi He[2,4*], and Huizhu Hu[1,5]

[1]Quantum Sensing Center, Zhejiang Lab, Hangzhou 310000, People's Republic of China
[2]State Key Laboratory of Precision Measuring Technology and Instruments, Tianjin University, Tianjin 300072, People's Republic of China
[3]Isvision (Hangzhou) Technology Co., Ltd., Hangzhou 310052, People's Republic of China
[4]Beijing Advanced Innovation Center for Soft Matter Science and Engineering, Beijing University of Chemical Technology, Beijing 100029, People's Republic of China
[5]State Key Laboratory of Modern Optical Instrumentation, College of Optical Science and Engineering, Zhejiang University, Hangzhou 310027, People's Republic of China

*E-mail: liuhaiqing@isv-tech.com; cghu@tju.edu.cn; czhe@mail.buct.edu.cn

Received March 29, 2022; revised April 10, 2022; accepted April 25, 2022; published online June 15, 2022

We researched the mechanical unfolding of protein domains in monomeric protein NuG2 and the tandem polyproteins $(NuG2)_8$ and $(NuG2)_{16}$ using a dual-trap optical tweezers system. By stretching NuG2 and its polyproteins, $(NuG2)_8$ and $(NuG2)_{16}$ at the constant pulling speed of 500 nm s^{-1}, we achieved the mechanical unfolding force of each domain in these proteins. Besides, we calculated the energy dissipation of NuG2, $(NuG2)_8$ and $(NuG2)_{16}$ by measuring the area enclosed by stretching and relaxation traces. Our results represent a key step towards engineering artificial polyproteins with controllable mechanical force and energy dissipation properties for force-buffering and energy dissipator applications.

Polyproteins formed by the covalent linkage of individual protein domains with different biological functions are widespread in nature.[1)] Tandem repeats of protein domains are significant in both natural and artificial materials, displaying unique mechanical responses.[2–8)] The giant titin protein is composed of hundreds of tandem linked Ig domains, which is essential to the function of muscle.[9–11)] The artificial polyprotein of GB1 is an ideal elastomeric protein with superior mechanical properties, which is anticipated to be applied to nanomechanical devices and/or constructing materials.[12–14)] Single-molecule force spectroscopy based on atomic force microscopy typically requires the use of polyprotein in order to provide fingerprints for unambiguous single-molecule events and improve the statistics of experiments data collection.[15–17)] Research on the viral polyprotein can not only help us understand the viral mechanisms, but also provide a theoretical basis for the drug design for the treatment of viral disease.[18–20)] Recent study also provided experimental evidence that stretching polyprotein in single-molecule optical tweezers was equivalent to stretching a single domain.[21)] Despite the extensive studies of polyprotein and applications of polyprotein in different fields, to the best of our knowledge, whether the individual domains in the polyprotein are of the same mechanical response has not been reported yet.

Atomic force microscopy, magnetic tweezers, and optical tweezers (OT), are the most widely used techniques in single-molecule force spectroscopy studies on biomolecules.[22–25)] Optical tweezers show good applicability in the measurement of protein force spectroscopy with its advantages of ultra-high resolution in force, spatial and time. In this work, we used single-molecule optical tweezers to study the mechanical unfolding of polyproteins in a different number of domains in both monomeric protein NuG2 and the tandem polyproteins $(NuG2)_8$ and $(NuG2)_{16}$. By stretching NuG2 and its polyproteins, $(NuG2)_8$ and $(NuG2)_{16}$ at the constant pulling speed of 500 nm s^{-1}, we achieved the mechanical unfolding force of each domain in these proteins. Besides, we calculated the energy dissipation of NuG2, $(NuG2)_8$ and $(NuG2)_{16}$ by measuring the area enclosed by stretching and relaxation traces. Our results indicate that the use of polyprotein enables the unfolding of mechanically stable proteins at relatively low forces and dramatically expands the range of the mechanical unfolding force, thus expanding the ranges of the force-buffering and the energy dissipation.

The experimental setup of dual-trap optical tweezers (DTOT) is shown in Fig. 1. A 1064 nm linearly polarized light beam (J20I-BL-106C, Spectra-Physics, 5 W) was used as a light source. To adjust the laser power, a half-wave plate was placed in front of the first polarization beam splitter (PBS1). By operating the computer-controlled motorized holder, the half-wave plate was rotated to realize the change in the output power. The adjusted light beam was split into two beams after PBS2. A two-axis piezoelectric mirror (PM, MTA2X HS, Mad City Labs) was used to reflect one of the beams with nano-radian resolution to control the 2D in-plane position of the trap in the focus plane. The other is modulated by an acousto-optic modulator and its frequency is shifted by 80 MHz to reduce the interference effect between the two beams. Then, two beams are brought into the first high numerical aperture microscope objective lens (OBJ, NA = 1.2, 63x, ZEISS) with the help of a telescope and a dichroic mirror, generating one movable trapping and one position-fixed trapping, respectively. The sample chamber was placed on a piezo-actuated translation stage (P-517.3 CL, Physik Instrumente). The condenser (NA = 1.2, 63x, ZEISS) behind the sample chamber was used to collect the transmitted light. The transmitted light then was separated by PBS4. To further carry out the force measurement, two-quadrant photodiode detectors at the end were used to monitor the two beams. A 780 nm LED was used as a light source and Kohler illumination was realized for a bright field imaging of the sample. Images of the sample were acquired by a charge-coupled device (CCD, DCC1545M, 25fps, Thorlabs).

The gene of monomeric NuG2, $(NuG2)_8$ and $(NuG2)_{16}$, which were kind gifts from Prof. Hongbin Li's group, were subcloned into a modified pET22b vector with a cysteine residue at N-terminus and an AviTag at C-terminus. The plasmid encoding Cys-NuG2-AviTag was co-transformed with pBirAcm into *E. coli* BL21(DE3) competent cells. The protein was then expressed and biotinylated in vivo by BirA

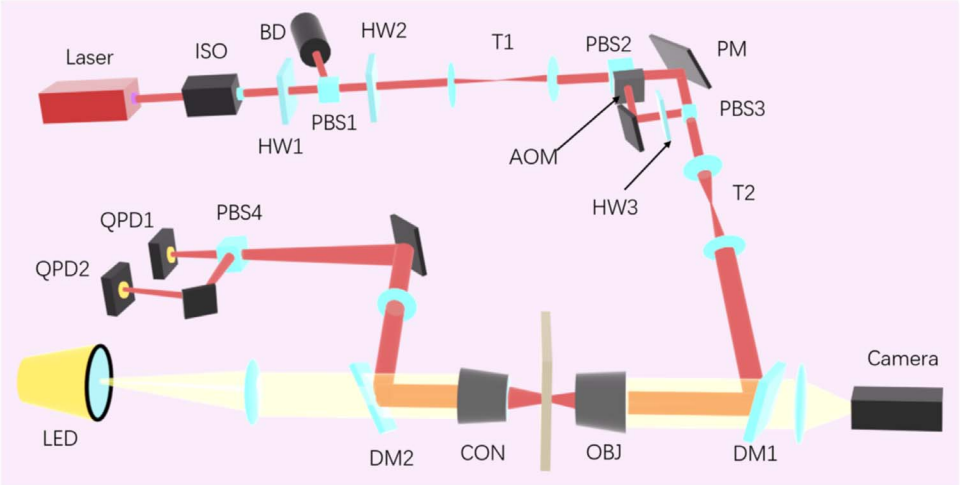

Fig. 1. (Color online) Schematic layout for DTOT (Laser, continuous-wave laser; HW, half-wave plate; PBS, polarizing beam splitter; BD, beam dump; AOM, acousto-optic modulator; PM, piezoelectric mirror; T, telescope; DM, dichroic mirror; OBJ, objective; SC, sample chamber; CON, condenser; QPD, quadrant photodiode; LED, light-emitting diode).

enzyme in *E. coli* BL21(DE3) strain with biotin added in the culturing media as reported. The protein Cys-NuG2-Biotin with C-terminal Histag was then purified by TALON metal affinity chromatography. Cys-$(NuG2)_8$-Biotin and Cys-$(NuG2)_{16}$-Biotin were prepared similarly.

The dsDNA handle of 802 base pairs was prepared by polymerase chain reaction (PCR) in a 96-well PCR plate using 5′ modified oligonucleotides, 5′Digoxigenin-CAAAAAACCCCTCAAGACCC (upstream) and 5′NH2-CGACGATAAACGTAAGGACATC (downstream), as primers and the pGEMEX-1plasmid as a template. The PCR product Dig-DNA-NH2 was precipitated by ice-cold ethanol and then dissolved to 2 μM using 1X PBS buffer (pH = 7.4). The Dig-DNA-NH2 was then allowed to react with 1 mM succinimidyl 4-(N-maleimidomethyl) cyclohexane-1-carboxylate (SMCC) to introduce a maleimide group, resulting in the Dig-DNA-Mal. Excess SMCC was removed by ethanol precipitation again and the Dig-DNA-Mal was dissolved to 2 μM in 1X PBS buffer (pH = 7.4) and stored at −80 °C.

The proteins carrying oane cysteine residue were diluted to 10 μM and reduced by 0.5 mM tris 2-carboxyethyl phosphine (TCEP) for 1 h before the coupling reaction. The excess TCEP was removed using Zeba desalting columns. Then 1 μl of 10 μM reduced proteins were then allowed to react with 1 μl of 2 μM Dig-DNA-MAL handle for 4 h at room temperature. The product, Dig-DNA-NuG2-Biotin, was purified using Qiagen PCR purification kits.

To perform single-molecule force spectroscopy experiments using DTOT, we mixed 5 ng of Dig-DNA-NuG2-Biotin with 1 μl of 0.1% AntiDig-coated polystyrene beads (diameter of ∼2 μm, from Spherotech) and wait 30 min. Then the same amount of streptavidin-coated polystyrene beads (diameter of ∼2 um, from Spherotech) was added together with the AntiDig beads into a glass chamber. DTOT was used to capture SA beads and AD beads and make the force-extension measurements at the speed of 500 nm s^{-1}.

We first investigated the feasibility of using DTOT to achieve the mechanical unfolding of polyproteins. The model system we chose here was a small a/b protein NuG2, whose mechanical unfolding was well studied by single-molecule force spectroscopy using both atomic force microscopy and single-beam optical tweezers.[21,26] The mixture of polyproteins and polystyrene beads was injected into the sample chamber, which was fixed on the sample stage of DTOT. When we use DTOT to perform single-molecule force spectroscopy experiments on NuG2 and its polyproteins, $(NuG2)_8$ and $(NuG2)_{16}$ at the constant pulling speed of 500 nm s^{-1}, the robust unfolding and refolding of NuG2 allowed

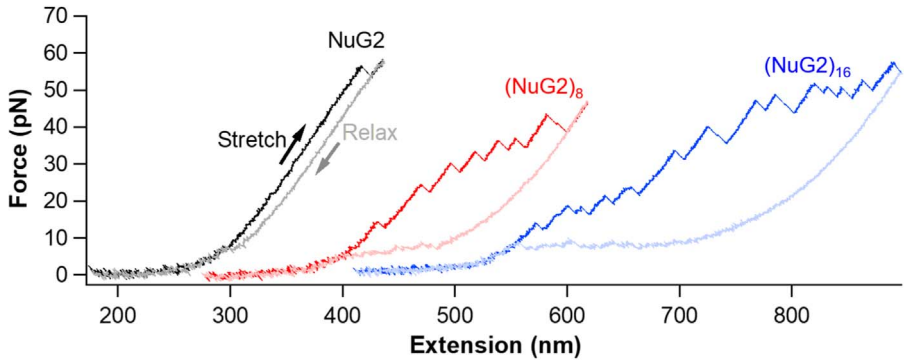

Fig. 2. (Color online) Representative force-extension curves of stretching and relaxing NuG2, $(NuG2)_8$ and $(NuG2)_{16}$ at the speed of 500 nm s^{-1}. The sudden force-decrease events on the stretching traces (in black) and the sudden force-increase events on the relaxing traces (in grey) correspond to the mechanical unfolding and refolding of individual NuG2 domains, respectively. The force-extension curves of $(NuG2)_8$ and $(NuG2)_{16}$ are colored in red and blue, respectively.

us to obtain the force-extension curves (FECs) effectively. As shown in Fig. 2, the two-state unfolding of NuG2 was observed at the rupture events. The saw-tooth-like pattern in the FECs provides evidence of pulling on a single molecule. Fitting the worm-like chain model of polymer elasticity to the rupture events revealed the contour length increment ΔLc of roughly 18 nm, which corresponded to the complete extensions of a single NuG2 domain and was consistent with the reported result.[27)]

To achieve the mechanical response of polyproteins, we first carry out the mechanical unfolding experiments of NuG2 monomer and deal with the force spectroscopy data. The model we used is Bell–Evans model,[28,29)] which can describe the mechanical unfolding of proteins:

$$k_u(F) = k_u(0)e^{\frac{F\Delta x_u}{k_b T}}, \quad (1)$$

where F is the applied force, k_b is the Boltzmann constant, T is the temperature in Kelvin, Δx_u is the unfolding distance between the native and the transition states, $k_u(F)$ and $k_u(0)$ are the unfolding rates at the force of F and zero, respectively. The unfolding force histogram of NuG2 monomer is shown in Fig. 3(A). The NuG2 displays high mechanical stability and it remains folded below 30 pN. To extract the mechanical unfolding kinetics, we transformed the unfolding force histogram into the unfolding rate versus applied force using the method previously reported by Dudko et al.[30)] Figure 3(B) shows the transformed results. Bell–Evans model was used to fit the results and the solid line is the linear fitting using the Bell–Evans model with the parameters of $k_u(0) = 0.013\ s^{-1}$ and $\Delta x_u = 0.66$ nm.

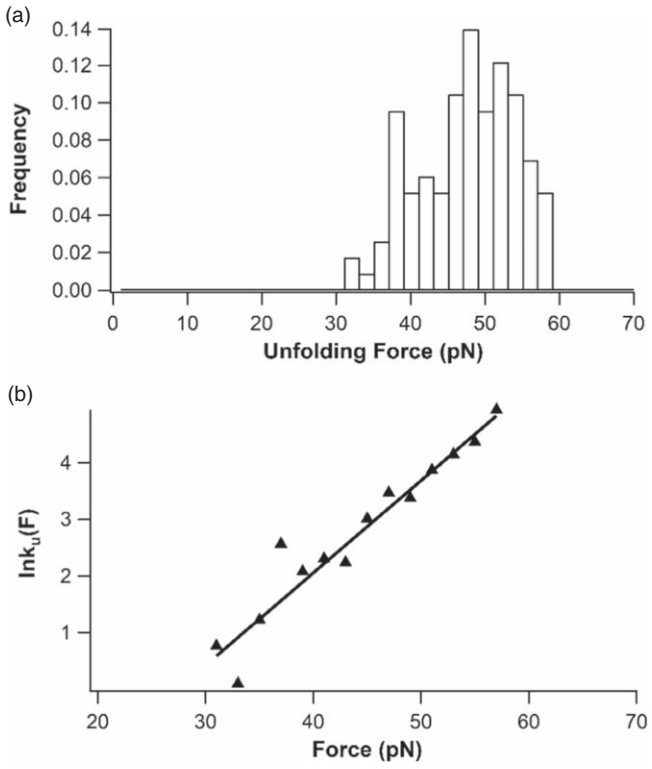

Fig. 3. (Color online) (A) Histogram of unfolding forces of NuG2 monomer. (B) The unfolding rates $k_u(F)$ as a function of the applied force F, obtained by transforming the unfolding force histogram in (A) according to the method previously reported by Dudko et al. The solid line is the linear fitting using the Bell–Evans model with the parameters of $k_u(0) = 0.013\ s^{-1}$ and $\Delta x_u = 0.66$ nm.

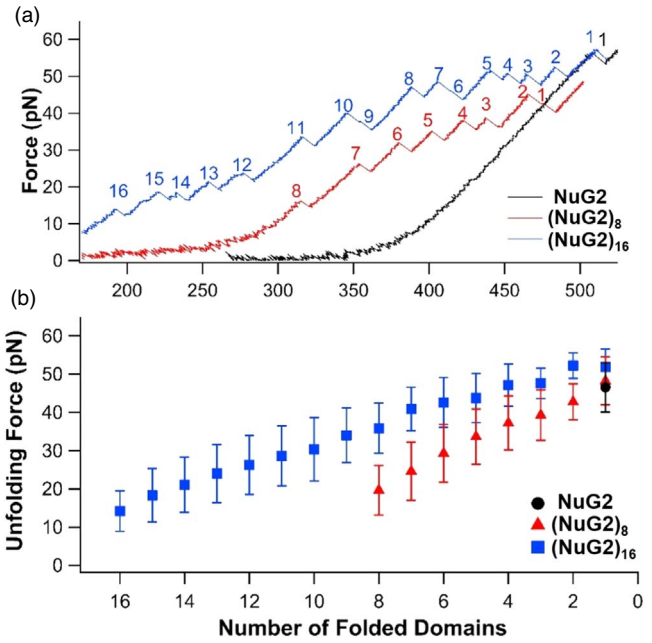

Fig. 4. (Color online) The unfolding forces of NuG2 in polyproteins increases as the number of folded domains decreases upon stretching. (A) Overlying of the unfolding traces of NuG2 (black), (NuG2)$_8$ (red) and (NuG2)$_{16}$ (blue). The numbers of folded domains before individual unfolding events are labeled above each unfolding force peaks. (B) The average unfolding forces at a different number of folded domains of NuG2, (NuG2)$_8$ and (NuG2)$_{16}$.

We then study the mechanical response of polyproteins of NuG2. We overlaid the stretching FECs of NuG2, (NuG2)$_8$ and (NuG2)$_{16}$ shown in Fig. 4(A). The number of folded domains before each unfolding event are labeled above the unfolding force peaks. The mechanical unfolding of NuG2 domain in polyproteins (NuG2)$_8$ and (NuG2)$_{16}$ was dramatically increased from roughly 10 pN to roughly 50 pN upon stretching, suggesting that the measured mechanical responses of individual domains vary in the polyprotein. However, the folding forces remain at roughly 8 pN, indicating that the number of domains does not have a major effect on the apparent folding force. To further figure out the difference between individual domains in polyproteins, we extracted the unfolding force histogram of each NuG2 domain in polyproteins (NuG2)$_8$ and (NuG2)$_{16}$ from the unfolding force spectroscopy data and calculated the unfolding force of each NuG2 domain by Gaussian fitting. Figure 4(B) shows the fitted results of the unfolding force of NuG2 monomer and its polyproteins versus the number of folded domains. It is clearly shown that the average unfolding forces of each NuG2 domain in polyproteins almost showed linear dependence on the number of folded domains before unfolding and the unfolding forces of the last domains in (NuG2)$_8$ and (NuG2)$_{16}$ are similar to the unfolding force of the single domain in NuG2 monomer. These results demonstrated that the use of polyprotein enables the unfolding of mechanically stable proteins at relatively low forces and dramatically expands the range of the mechanical unfolding force, thus the polyproteins can serve as force-buffer.

Finally, based on our force spectroscopy results, we calculated the energy dissipation of individual domains in NuG2, (NuG2)$_8$ and (NuG2)$_{16}$. Different from the method used by atomic force microscopy,[31)] the approach we used

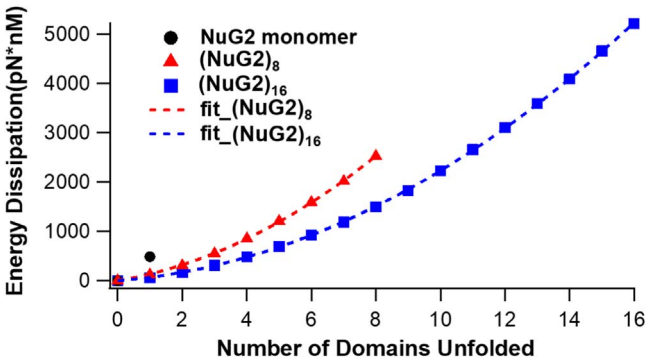

Fig. 5. (Color online) Energy dissipation of NuG2, $(NuG2)_8$ and $(NuG2)_{16}$ upon stretching and relaxation. The relationship of energy dissipation and number of domains unfolded can be fitted using $\text{Energy} = 109.4 * N + 25.8 * N^2$ for $(NuG2)_8$ and $\text{Energy} = 50.1 * N + 17.3 * N^2$ for $(NuG2)_{16}$, N represents the number of domains unfolded.

here is a direct, model-free integration of the observed FEC. Thanks to the fact that the force spectrum data based on optical tweezers has both unfolding and folding curves, we could directly calculate the energy dissipation of polyproteins by measuring the area enclosed by stretching and relaxation traces. As shown in Fig. 5, it clearly showed that the energy dissipation increases in a nonlinear fashion as the number of domains unfolded increases. The relationship of energy dissipation and number of domains unfolded can be fitted using $\text{Energy} = 109.4 * N + 25.8 * N^2$ for $(NuG2)_8$ and $\text{Energy} = 50.1 * N + 17.3 * N^2$ for $(NuG2)_{16}$, where N represents the number of domains unfolded. This nonlinear dependency is due to the unfolding force increasing as the individual domains unfold upon stretching while the folding force remain almost the same. These results demonstrated that the polyproteins can serve as the energy dissipater.

In conclusion, our results suggest that the multiple domains in polyprotein effectively reduced the unfolding force of a mechanical stable protein NuG2 from roughly 40 pN to roughly 10 pN (the first unfolding event in a stretching curve). Our results are useful in studying the mechanical response of protein-based materials. The unfolding and refolding of proteins are responsible for energy dissipation when the protein-based materials are stretched and relaxed. The protein can serve as the energy dissipater and force-buffer. The use of polyprotein enables the unfolding of mechanically stable proteins at relatively low forces and dramatically expands the range of the mechanical unfolding force, thus highlighting the potential versatility of polyproteins that can be used in force-buffering and energy dissipation.

Acknowledgments The authors thank Prof. Hongbin Li at the University of British Columbia for fruitful discussions. This study was supported by National Natural Science Foundation of China (NO. 11902023, NO.61223008), National Key Research and Development Program of China (No. 2021YFC2103903), Natural Science Foundation of Tianjin City (NO. 15JCZDJC31600), Open Project Fund (pilab1902) of the State Key Laboratory of Precision Measuring Technology and Instruments (Tianjin University), and Major Scientific Research Project of Zhejiang Laboratory (2019MB0AD01).

ORCID iDs Huizhu Hu https://orcid.org/0000-0003-1690-9414

1) T. Crépin, C. Swale, A. Monod, A. Monod, F. Garzoni, M. Chaillet, and I. Berger, Curr. Opin. Struct. Biol. **32**, 139 (2015).
2) T. A. Bharat, L. R. C. Menendez, W. J. Hagen, V. Lux, S. Igonet, M. Schorb, F. K. M. Schur, H. G. Kräusslich, and J. A. G. Briggs, Proc. Natl. Acad. Sci. **111**, 8233 (2014).
3) Y. Cao, M. Balamurali, D. Sharma, and H. B. Li, Proc. Natl. Acad. Sci. **104**, 15677 (2007).
4) J. Konvalinka, H. G. Kräusslich, and B. Müller, Virology **479**, 403 (2015).
5) L. Li, H. H. L. Huang, C. L. Badilla, and J. M. Fernandez, J. Mol. Biol. **345**, 817 (2005).
6) F. K. M. Schur, W. J. H. Hagen, M. Rumlová, T. Ruml, B. Müller, H. G. Kräusslich, and J. A. G. Briggs, Nature **517**, 505 (2015).
7) C. C. Wang, T. Y. Tsong, Y. H. Hsu, and P. E. Marszalek, Biophys. J. **100**, 1094 (2011).
8) H. Dietz, M. Bertz, M. Schlierf, F. Berkemeier, T. Bornschlögl, J. P. Junker, and M. Rief, Nat. Protocols **1**, 80 (2006).
9) E. C. Eckels, R. Tapia-Rojo, J. A. Rivas-Pardo, and J. M. Fernandez, Annu. Rev. Physiol. **80**, 327 (2018).
10) A. L. Hessel, S. L. Lindstedt, and K. C. Nishikawa, Front. Physiol. **8**, 70 (2017).
11) J. A. Rivas-Pardo, E. C. Eckels, I. Popa, P. Kosuri, W. A. Linke, and J. M. Fernandez, Cell. Rep. **14**, 1339 (2016).
12) Y. Cao and H. B. Li, Nat. Mater. **6**, 109 (2007).
13) H. Lei et al., Nat. Commun. **11**, 4032 (2020).
14) S. S. Lv, D. M. Dudek, Y. Cao, M. M. Balamurali, J. Gosline, and H. B. Li, Nature **465**, 69 (2010).
15) F. Benedetti, C. Micheletti, G. Bussi, S. K. Sekatskii, and G. Dietler, Biophys. J. **101**, 1504 (2011).
16) T. Hoffmann and L. Dougan, Chem. Soc. Rev. **41**, 4781 (2012).
17) F. Sumbul, A. Marchesi, and F. Rico, J. Chem. Phys. **148**, 123335 (2018).
18) F. I. L. Hucke and J. J. Bugert, Front. Public Health **8**, 916 (2020).
19) C. T. T. Su, C. K. Kwoh, C. S. Verma, and S. K. E. Gan, J. Biomol. Struct. Dyn. **36**, 4366 (2018).
20) P. Anand, P. J. Lenehan, M. Niesen, U. Yoo, D. Patwardhan, M. Montorzi, A. J. Venkatakrishnan, and V. Soundararajan, Cell Death Discovery **8**, 124 (2022).
21) H. Lei, C. Z. He, C. G. Hu, J. L. Li, X. D. Hu, X. T. Hu, and H. B. Li, Angew. Chem. Int. Edit. **56**, 6117 (2017).
22) K. C. Neuman and A. Nagy, Nat. Meth. **5**, 491 (2008).
23) M. L. Hughes and L. Dougan, Rep. Prog. Phys. **79**, 076601 (2016).
24) J. S. Zhang, H. Lei, M. Qin, W. Wang, and Y. Cao, Supramol. Mater. **1**, 100005 (2022).
25) W. S. Di, X. Wang, Y. Y. Zhou, Y. H. Mei, W. Wang, and Y. Cao, Chin. Phys. Lett. **39**, 038701 (2022).
26) C. Z. He, C. G. Hu, X. D. Hu, X. T. Hu, A. Xiao, T. T. Perkins, and H. B. Li, Angew. Chem. Int. Edit. **54**, 9921 (2015).
27) A. Xiao and H. B. Li, Chem. Commun. **55**, 12920 (2019).
28) G. I. Bell, Science **200**, 618 (1978).
29) E. Evans, Annu. Rev. Biophys. Biomol. Struct. **30**, 105 (2001).
30) O. K. Dudko, G. Hummer, and A. Szabo, Proc. Natl. Acad. Sci. **105**, 15755 (2008).
31) J. B. Thompson, H. G. Hansma, P. K. Hansma, and K. W. Plaxco, J. Mol. Biol. **322**, 645 (2002).